Proposed AASHTO guidelines for adjacent precast concrete box beam bridge systems, part 1: Analytical investigation

Abdullah Haroon, Waleed Hamid, Richard Miller, Bahram Shahrooz, and Eric Steinberg

- This study reviewed shear key configurations for adjacent box-girder bridges using precast concrete hollow boxes.
- The objective of the study was to mitigate leakage problems in adjacent box-girder bridges and provide recommendations to improve the load-transfer mechanism between them.
- Using finite element analysis software, a total of 48 models were developed to investigate joint performance when subjected to thermal and live loads. The effectiveness of post-tensioning and shear key reinforcement in mitigating shear key cracking was assessed.

Adjacent box-girder bridges provide a low-cost solution for short-span bridges, especially when a shallow bridge profile is required. The girder cross section consists of precast concrete hollow boxes that are erected side by side to form a bridge profile. The load between the adjacent girders is transferred using shear keys, which are typically placed near the top of the section. At certain points along the length of the girder, the voids are omitted to create diaphragms. Threaded rods are passed through holes in the diaphragms, typically below the level of the shear key but above the neutral axis of the section. Tightening the nuts on these rods pulls the girders together and helps with load transfer, even if shear keys are compromised. The shear keyways are cast, usually with a nonshrink, prepackaged grout.

However, the problem with these bridges is that the shear keys crack, causing leakage and, in some cases, loss of load transfer. The cracked shear key can allow salt-laden water to penetrate the girders and lead to corrosion of the strands and deterioration of the girders. The performance of these bridges could be greatly improved if cracking in joints could be eliminated while maintaining the needed load-transfer capabilities.

Huckelbridge, El-Esnawi, and Moses[1] showed that the keys can tolerate some cracking and still transfer load, but there have been documented cases where shear key deterioration was so bad that load transfer was lost. Loss of load transfer is not acceptable because load distribution between beams

is assumed in design. Adjacent box girders have live-load moment-distribution factors of about 0.30. Without load transfer, considering the typical girder width, this factor increases to 0.50. However, there is evidence that shear keys are less important for load transfer. As noted by Russell,[2] the typical design of an adjacent box-girder bridge uses lateral tie rods. These rods may be prestressed to compress the joint or may be simply hand tightened to pull the girders together. Fuentes[3] and Steinberg et al.[4] showed that even untensioned tie rods will transfer loads. El-Remaily et al.[5] and Hussein[6] indicate that transverse rods alone can be used for load transfer and shear keys can be eliminated.

While loss of load transfer is an issue, the far bigger problem is leakage of the joints. Cracking in the shear key joints is likely caused by temperature and shrinkage. Huckelbridge, El-Esnawi, and Moses[1] studied shear keys being replaced in an existing bridge. The authors found the keys cracked almost immediately but were not sure why. Miller et al.[7] found that the most likely reason was temperature-induced movements. Miller and his coauthors noted that the cracks formed within one week and that the cracks opened and closed with daily temperature cycles. Sharpe[8] conducted an analytical study using Texas Department of Transportation girders. This study confirmed that temperature and shrinkage cause initial cracking. Most recently, Ulku et al.[9] and Hussein et al.[10] further confirmed this behavior. Miller et al.[7] and Sharpe[8] found that cracks tend to start near the ends of the girders. However, a recent study by Graybeal[11] did not find significant cracking when a temperature gradient of 50°F (28°C) was applied. Stresses from live loads do not appear to cause the cracks, but simply propagate temperature-induced cracks. This effect was confirmed by Miller et al.,[7] Sharpe,[8] Grace et al.,[12] and Hussein et al.[10] Graybeal[11] noted that even severe, cyclic loading did not crack intact shear keys.

The research presented in this paper is a portion of a larger study performed under the National Cooperative Highway Research Program (NCHRP) project 12-95A. The objective of the study was to mitigate the leakage problem in adjacent box-girder bridges while at the same time providing recommendations to improve the load-transfer mechanism between them. The overall project consisted of several phases, which included a comprehensive analytical study followed by full-scale experimental testing. Only the analytical portion of the study is discussed in this paper. The analytical findings guided the direction of a full-scale experimental testing program, which will be the subject of a companion paper.

Types of shear keys

The shape and location of the shear key are critical, as they can affect the stress profile of the shear key and therefore help mitigate cracking. Traditionally, the shear key is located near the top of the girder section. There is no record of any design methodology for the original shear key shape. Most states that use adjacent box-girder bridges still use some variation of this original shear key shape and it is a "standard detail" with no associated design calculations.[2] Several authors[5,13–17] recommend full-depth shear keys. Evidence from Dong[14] indicates that this configuration is favorable because it changes the direction of principal stress from lateral to longitudinal. Another possibility is using a middepth shear key. A middepth shear key was used on a high-performance concrete bridge in Ohio when experimental evidence suggested it was less susceptible to temperature-induced cracking.[18] This shear key was cast only at middepth and the area above the key was not filled with grout. It was filled with compacted sand.

Based on evidence in the literature, four different shear key configurations were tested (**Fig. 1**). Figure 1 shows the tra-

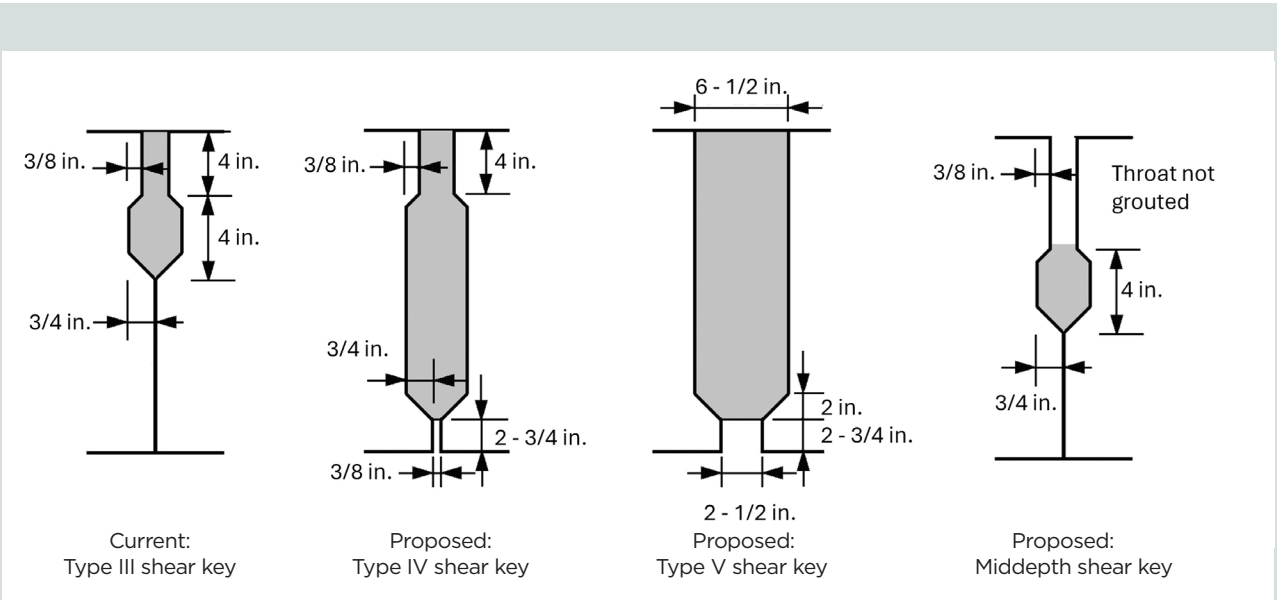

Figure 1. Shear key configurations. Note: 1 in. = 25.4 mm.

ditional top, partial-depth shear key (often called a Type III). The dimensions shown are an "average" of the shear keys used in Ohio, Indiana, Michigan, and Kentucky. Figure 1 also shows possible full-depth shear keys, called Type IV and Type V. Research suggests these are more resistant to cracking due to a higher bond area and most of the shear key being outside of the zone of severe temperature gradient. Type IV has the same throat as Type III; however, the cutout has been extended to the bottom of the girder. Type V has a 6.5 in. (165 mm) throat that extends uniformly to the bottom of the girder. Last, Fig. 1 shows the partially grouted middepth shear key tried in a bridge in Ohio. The key dimensions are the same as those of a Type III shear key but moved to the middepth of the girder.

Analytical program

The finite element analysis was performed using finite element analysis software to simulate the adjacent precast, prestressed concrete box-girder bridges. The model was generated to evaluate the effect of temperature gradient on various shear key configurations. Elastic material models were assigned to box concrete, grout, and steel reinforcement. In addition, the coefficients of thermal expansion for the materials were also assigned to simulate the performance of the bridge components under temperature fluctuations. All of the bridge components, except the tie rod, were modeled using eight-node (C3D8R) linear brick elements with reduced integration. The partition option in the finite element analysis software was used at various locations to simplify the geometry, helping to achieve a more uniform mesh size. A finer mesh was used in and around the shear keys to enhance the accuracy of modeling the interface behavior between the shear keys and girders. Mesh sizes from 4 to 8 in. (101.6 to 203.2 mm) were used in the entire model. A tie constraint using the surface-to-surface model was used to define the interaction of the longitudinal interface between the shear key and box girder.

A comprehensive analytical program was performed with the following objectives:

- to assess the stresses in various shear key configurations under temperature movements
- to assess the stresses in various shear key configuration under live load application
- to determine parameters that affect shear key performance (parameters considered were span length, girder depth, skew, deck type, amount of lateral post-tensioning, and keyway reinforcement)

Bridge model details

A total of 48 separate models (labeled cases 1 through 48) were developed. The model cross section consisted of seven 48 in. (1219 mm) wide box girders. Decks, either asphalt or concrete, were taken as 6 in. (152 mm) thick. The first 28 models (cases 1 through 28) were various configurations of spans, girder depths, shear key types, and decks without lateral post-tensioning. These models were analyzed for temperature stresses and live-load stresses. The next 16 models (cases 29 through 44) were various configurations of spans, girder depths, shear key types, and decks with lateral post-tensioning. These models were analyzed under a combination of thermal and post-tensioning stresses. The final four models (cases 45 through 48) had reinforced shear keys and were analyzed to assess the effectiveness of keyway reinforcement. The bridge models were simply supported at the ends on bearing pads that were 9 × 6 × 1 in. (228.6 × 152.4 × 25.4 mm). The 9 in. dimension was placed transverse to the bridge span. One end of the girders had two bearing pads and the other end of the girders had a single centered bearing pad. This was done to investigate the effects of using a single center bearing pad compared with two bearing pads placed near the edges of the girder. **Figure 2** shows the bridge cross section and girder assembly for each representative model case. **Table 1** provides a summary of the bridge models considered.

Unless noted otherwise, the material properties were as shown in **Table 2**. Grout properties were determined as the typical properties of nonshrink grout materials listed on the Ohio Department of Transportation's approved product list in flowable condition.

Temperature analysis of the shear keys

Temperature movements are suspected to cause cracking in shear keys within the first few days after grouting. During the day, the top of the girder is exposed to sun and gets hot, whereas the bottom of the girder remains cool. This generates a temperature gradient though the girder depth that generates lateral and transverse stresses in shear keys. For the analysis of these stresses, the American Association of State Highway and Transportation Officials (AASHTO) specifies a thermal gradient though the depth of the girder.[19] For this purpose, it divides the country into four zones depending on the severity of the temperature variations. The thermal gradient depends on the location of the bridge, the depth of the bridge, and the material type. The thermal gradient through the depth of the girder for concrete bridges can be defined as shown in **Fig. 3**, where T_1 and T_2 are the temperature gradients that depend on the zone. For the most extreme case of zone 1, the values of T_1 and T_2 are 54°F (30°C) and 14°F (8°C), respectively. Temperature T_3 should be taken as zero unless field determined; however, it should not exceed 5°F (3°C). The dimension A depends on the depth of the girder and is taken as 12 in. (304.8 mm) for girders 16 in. (406.4 mm) and deeper and is taken as 4 in. (101.6 mm) for a girder depth shallower than 16 in.

Field data shows that the cracks tend to start near the ends of the girders.[7,20] This may be due to some restraint from the end bearings. Therefore, to see the effect of the end restraint, bridge models were supported on a single bearing pad on one

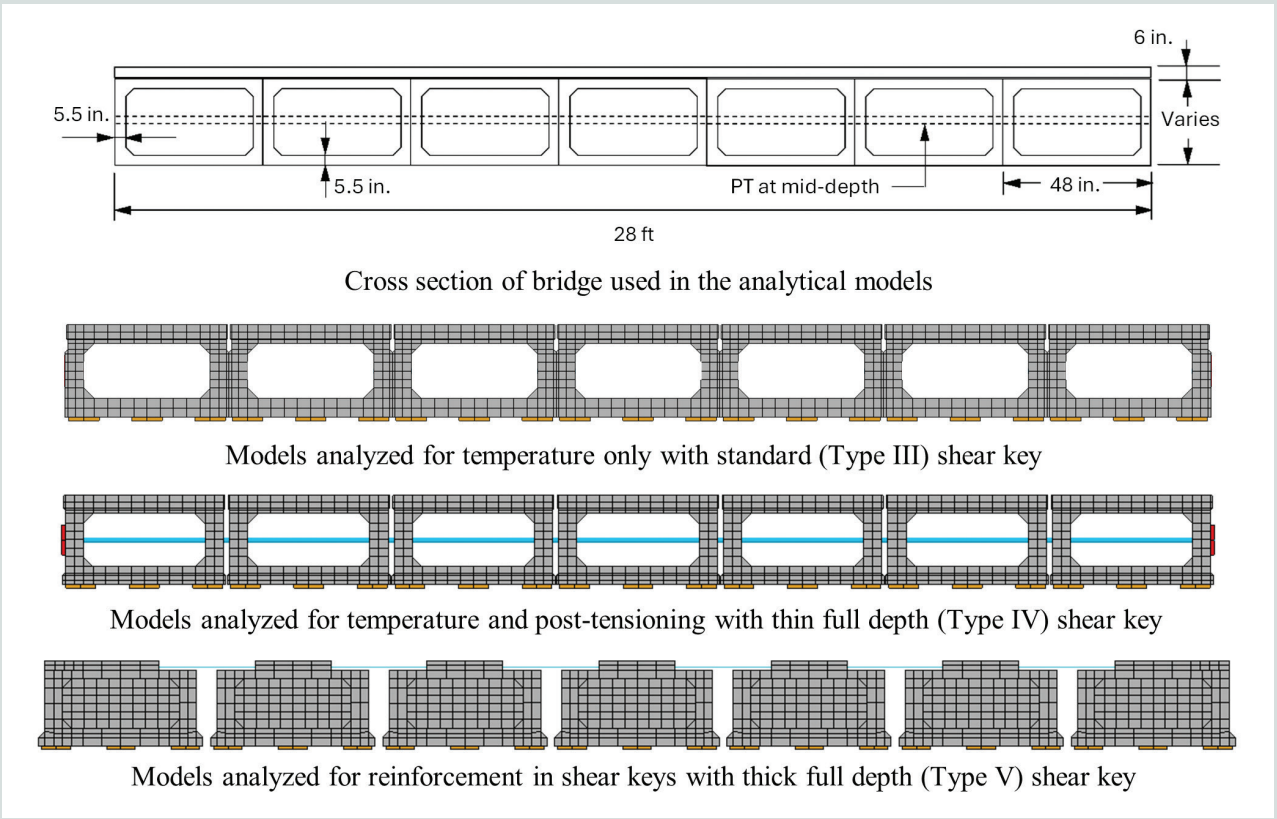

Figure 2. Girder assembly for bridge models used in analytical modeling. Note: PT = post-tensioning. 1 in. = 25.4 mm; 1 ft = 0.305 m.

Table 1. Bridge models used in the analytical study

Case	Span, ft	Girder depth, in.	Shear key	Deck	Skew, degrees	Post-tensioning locations	Post-tensioning stress, ksi
1	45	27	Type III	concrete	0	none	none
2	60	27	Type III	concrete	0	none	none
3	60	42	Type III	concrete	0	none	none
4	80	42	Type III	concrete	0	none	none
5	45	27	Type IV	concrete	0	none	none
6	60	27	Type IV	concrete	0	none	none
7	60	42	Type IV	concrete	0	none	none
8	80	42	Type IV	concrete	0	none	none
9	45	27	Type V	concrete	0	none	none
10	60	27	Type V	concrete	0	none	none
11	60	42	Type V	concrete	0	none	none
12	80	42	Type V	concrete	0	none	none
13	45	27	middepth	concrete	0	none	none
14	60	27	middepth	concrete	0	none	none

Table 1 continued on p. 41

Table 1 continued from p. 40

Table 1. Bridge models used in the analytical study

Case	Span, ft	Girder depth, in.	Shear key	Deck	Skew, degrees	Post-tensioning locations	Post-tensioning stress, ksi
15	60	42	middepth	concrete	0	none	none
16	80	42	middepth	concrete	0	none	none
17	60	27	Type III	asphalt	0	none	none
18	60	27	Type IV	asphalt	0	none	none
19	60	27	Type V	asphalt	0	none	none
20	60	27	middepth	asphalt	0	none	none
21	60	27	Type III	concrete	30	none	none
22	60	27	Type IV	concrete	30	none	none
23	60	27	Type V	concrete	30	none	none
24	60	27	middepth	concrete	30	none	none
25	80	42	Type III	concrete	30	none	none
26	80	42	Type IV	concrete	30	none	none
27	80	42	Type V	concrete	30	none	none
28	80	42	middepth	concrete	30	none	none
29	45	27	Type III	concrete	0	ends and midspan	93
30	60	27	Type III	concrete	0	ends and thirds	102
31	80	42	Type III	concrete	0	ends and quarters	106
32	45	27	Type IV	concrete	0	ends and midspan	93
33	60	27	Type IV	concrete	0	ends and thirds	102
34	80	42	Type IV	concrete	0	ends and quarters	106
35	45	27	Type V	concrete	0	ends and midspan	93
36	60	27	Type V	concrete	0	ends and thirds	102
37	80	42	Type V	concrete	0	ends and quarters	106
38	45	27	middepth	concrete	0	ends and midspan	93
39	60	27	middepth	concrete	0	ends and thirds	102
40	80	42	middepth	concrete	0	ends and quarters	106
41	60	27	Type III	asphalt	0	ends and thirds	102
42	60	27	Type IV	asphalt	0	ends and thirds	102
43	60	27	Type V	asphalt	0	ends and thirds	102
44	60	27	middepth	asphalt	0	ends and thirds	102
45	60	27	Type III reinforced	asphalt	0	none	none
46	60	42	Type III reinforced	asphalt	0	none	none
47	60	27	Type V reinforced	asphalt	0	none	none
48	60	42	Type V reinforced	asphalt	0	none	none

Note: 1 in. = 25.4 mm; 1 ft = 0.305 m; 1 ksi = 6.895 MPa.

Table 2. Material properties of various bridge model components

Property	Girder concrete	Deck concrete	Grout	Steel
Compressive strength, ksi	6	4.5	3 ksi at 1 day, 8 ksi at 28 days	n.d.
Modulus of elasticity, ksi	4500	3800	3000	29,000
Poisson's ratio	0.2	0.2	0.2	0.28
Tensile strength, psi	590	500	600	60,000
Coefficient of thermal expansion, °F	5.5×10^{-6}	5.5×10^{-6}	5.5×10^{-6}	6.0×10^{-6}

Note: n/d = no data. °F = (°C × 1.8) + 32; 1 psi = 6.895 kPa; 1 ksi = 6.895 MPa.

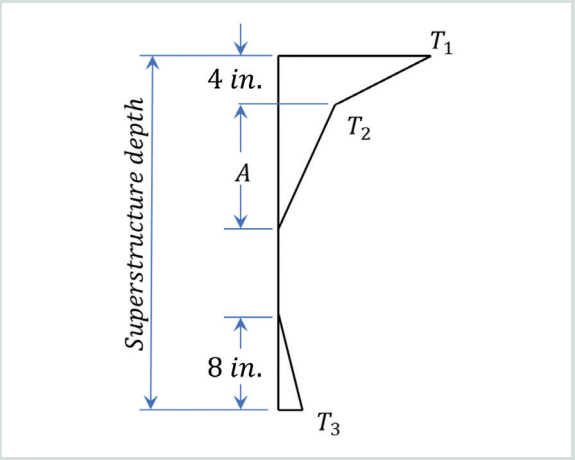

Figure 3. AASHTO thermal gradient profile. Note: *A* = dimension dependent on depth of girder (12 in. for girder depths ≥16 in. and 4 in. for girder depths < 16 in.); AASHTO = American Association of State Highway and Transportation Officials; T_1 = temperature gradient for zone 1; T_2 = temperature gradient for zone 2; T_3 = temperature gradient for zone 3. 1 in. = 25.4 mm.

end whereas two bearing pads were used on the other end.

The temperature modeling was handled as follows:

1. The bridge was modeled. The shear keys and concrete deck (for models with a concrete deck) were present but were turned off to allow the elements to follow the deformations of the girders.

2. The AASHTO temperature gradient for zone 1 was applied to the box girders. This caused the top of the boxes to expand.

3. The shear key and deck material were then turned on to simulate the casting of the shear keys and deck. For asphalt decks, the asphalt was not modeled but the weight was added.

4. The temperature gradient was then removed from the girder to simulate cooling of the girders.

5. Stresses in the girders and keys were then assessed after cooling.

The maximum shear key stresses due to temperature loading for cases 1 to 28 are provided in **Table 3**. The maximum stresses typically occurred at the end of the girders supported with two bearing pads (location II) compared with the end with a single bearing pad (location I). In most cases, the difference in the stresses on each end was minor. The transverse stresses in the shear keys were higher than the longitudinal stresses. This agrees what has often been observed in the field with cracking occurring longitudinally due to transverse stress.

The maximum transverse stress in the shear keys increased with the span length and girder depth for the Type III and Type V shear keys. However, the maximum transverse shear key stresses decreased with the span and beam depth for the Type IV shear key. There was little change for the middepth shear key.

When the concrete deck was replaced with an asphalt wearing surface, the maximum transverse stress in the shear keys increased for all shear key types except for Type V, which had negligible change. Of note was the large increase in stress in the middepth shear key. It appeared this key is more vulnerable to stresses when the deck is not present.

Increasing the skew of the bridge to 30 degrees resulted in maximum transverse stress increases for the Type IV and middepth shear keys but reductions in maximum transverse stresses in the Type III and Type V shear keys.

Though the maximum stresses provided valuable information, it is important to get a more complete picture of the behavior of the joints when subjected to heating and cooling. The top image of **Fig. 4** provides the transverse shear stress in the exterior and first two interior Type III shear keys near the end of case 2. Note that, for clarity, this figure and following figures only show the shear keys and no girders. As shown in the top image, high transverse tensile stress exists near the top of the key at the ends. This stress is in the range of 900 psi (6206 kPa), which is sufficient to crack the shear key. Also, the transverse stress remained tensile throughout the depth of the shear key at the ends. Moving away from the ends toward midspan shows the transverse stress becoming compressive.

Table 3. Maximum stress in shear keys for all cases

Case	Shear key	Analysis type	Post-tensioning location	Maximum transverse stress		Maximum longitudinal stress	
				Value, ksi	Location*	Value, ksi	Location*
1	Type III	thermal stresses only	n/a	0.73	II	0.54	II
2	Type III		n/a	0.96	II	0.60	I
3	Type III		n/a	1.00	II	0.75	II
4	Type III		n/a	1.00	II	0.75	II
5	Type IV		n/a	0.97	II	0.72	II
6	Type IV		n/a	0.74	II	0.54	II
7	Type IV		n/a	0.69	II	0.55	II
8	Type IV		n/a	0.69	II	0.60	II
9	Type V		n/a	0.82	II	0.64	II
10	Type V		n/a	0.82	II	0.63	I
11	Type V		n/a	0.93	II	0.52	II
12	Type V		n/a	1.02	II	0.63	II
13	middepth		n/a	0.83	II	0.24	II
14	middepth		n/a	0.87	II	0.28	II
15	middepth		n/a	0.82	II	0.20	II
16	middepth		n/a	0.76	II	0.22	II
17	Type III		n/a	1.25	I	0.37	I
18	Type IV		n/a	1.13	II	0.63	II
19	Type V		n/a	0.78	II	0.43	II
20	middepth		n/a	2.13	II	0.40	II
21	Type III		n/a	0.69	II	0.60	II
22	Type IV		n/a	0.94	II	0.77	II
23	Type V		n/a	0.63	II	0.56	II
24	middepth		n/a	1.13	II	0.30	II
25	Type III		n/a	0.67	II	0.60	II
26	Type IV		n/a	0.93	II	0.78	II
27	Type V		n/a	0.55	II	0.53	II
28	middepth		n/a	1.19	II	0.35	II
29	Type III	thermal and post-tensioning stresses	ends and midspan	0.60	I	0.55	I
30	Type III		ends and thirds	0.88	I	0.69	I
31	Type III		ends and quarters	1.32	I	0.87	I
32	Type IV		ends and midspan	0.88	II	0.72	II
33	Type IV		ends and thirds	0.61	II	0.52	II
34	Type IV		ends and quarters	0.59	II	0.55	II
35	Type V		ends and midspan	0.73	II	0.62	II

Table 3 continued on p. 44

Table 3 continued from p. 43

Table 3. Maximum stress in shear keys for all cases

Case	Shear key	Analysis type	Post-tensioning location	Maximum transverse stress		Maximum longitudinal stress	
				Value, ksi	Location*	Value, ksi	Location*
36	Type V	thermal and post-tensioning stresses	ends and thirds	0.73	II	0.62	II
37	Type V		ends and quarters	0.56	II	0.51	II
38	middepth		ends and midspan	0.66	MID	0.19	MID
39	middepth		ends and thirds	0.68	MID	0.22	MID
40	middepth		ends and quarters	0.63	MID	0.19	MID
41	Type III		ends and thirds	0.84	II	0.34	MID
42	Type IV		ends and thirds	0.68	II	0.47	II
43	Type V		ends and thirds	0.72	II	0.36	II
44	middepth		ends and thirds	0.56	II	0.11	II
45	Type III reinforced	thermal stresses only	n/a	0.90	II	0.78	II
46	Type III reinforced		n/a	0.91	II	0.81	II
47	Type V reinforced		n/a	0.94	II	0.79	I
48	Type V reinforced		n/a	0.92	II	0.82	II

* Location of maximum stress: I = near single bearing pad end; II = near two bearing pad end; MID = at the midspan.

Note: n/a = not applicable. 1 ksi = 6.895 MPa.

Again, this is consistent with field observations of cracking starting near the end of the girders.

The middle image in Fig. 4 shows the transverse shear key stresses for the Type IV key for case 6. As shown, the stresses were high in the throat of the key and in the range of 700 psi (4827 kPa). However, the stresses decreased with depth of the key and compressive stresses existed at the bottom of the key near the end. This implies that cracking was still likely to occur near the top but may not fully penetrate through the full depth of the key. In addition, tensile stresses approximately less than 300 psi (2069 kPa) existed at the base of the throat of the key.

The bottom image in Fig. 4 provides the results for the transverse shear key stresses of the Type V key for case 10. Like the Type IV key, the stresses were high near the top and exceeded 800 psi (5516 kPa). However, the transverse stresses at the bottom of the key were compressive even at the very end of the key. This suggested that the full-depth shear key may be successful because cracking will not penetrate the entire depth of the shear key, and this may prevent leakage.

Temperature analysis of shear keys where throat is not grouted

Removing the grout material within the shear key throat was also investigated. This simulates two cases: either the throat is cracked and unable to transfer load or the throat is simply not grouted. The results for Type IV without the shear key throat being grouted are shown in the top image of **Fig. 5.** The transverse stresses were highly tensile near the top but dropped significantly and quickly with depth, eventually turning to compression. This was consistent with previous research by Huckelbridge et al.[1] indicating that cracking starts in the throat and that removing the throat grout (as is done in the middepth shear key) may prevent cracking. In this configuration, the throat could be filled with a filler or sealer material, which may help prevent leakage.

The bottom image of Fig. 5 shows the transverse shear key stresses for the middepth key (which was originally proposed without a grouted throat). Similar to the Type IV key, the stresses were high at the top of the key (about 900 psi [6206 kPa]) and dropped quickly with depth. By the midpoint of the key, the tensile stresses were nearly zero and small compressive stresses developed at the bottom of the middepth shear key. As with the full-depth shear keys, the results suggested these keys may crack near the top, but the cracks may not propagate the entire depth of the shear key.

Although not explicitly modeled, the bottom image of Fig. 4 suggested that a Type V key would have little or no tensile stress if the key were not completely filled with grout or if cracking occurred at the top of key. Also, the top image of Fig. 4 suggested that removing the grout from the throat of a Type III key would be ineffective because the entire key is in tension.

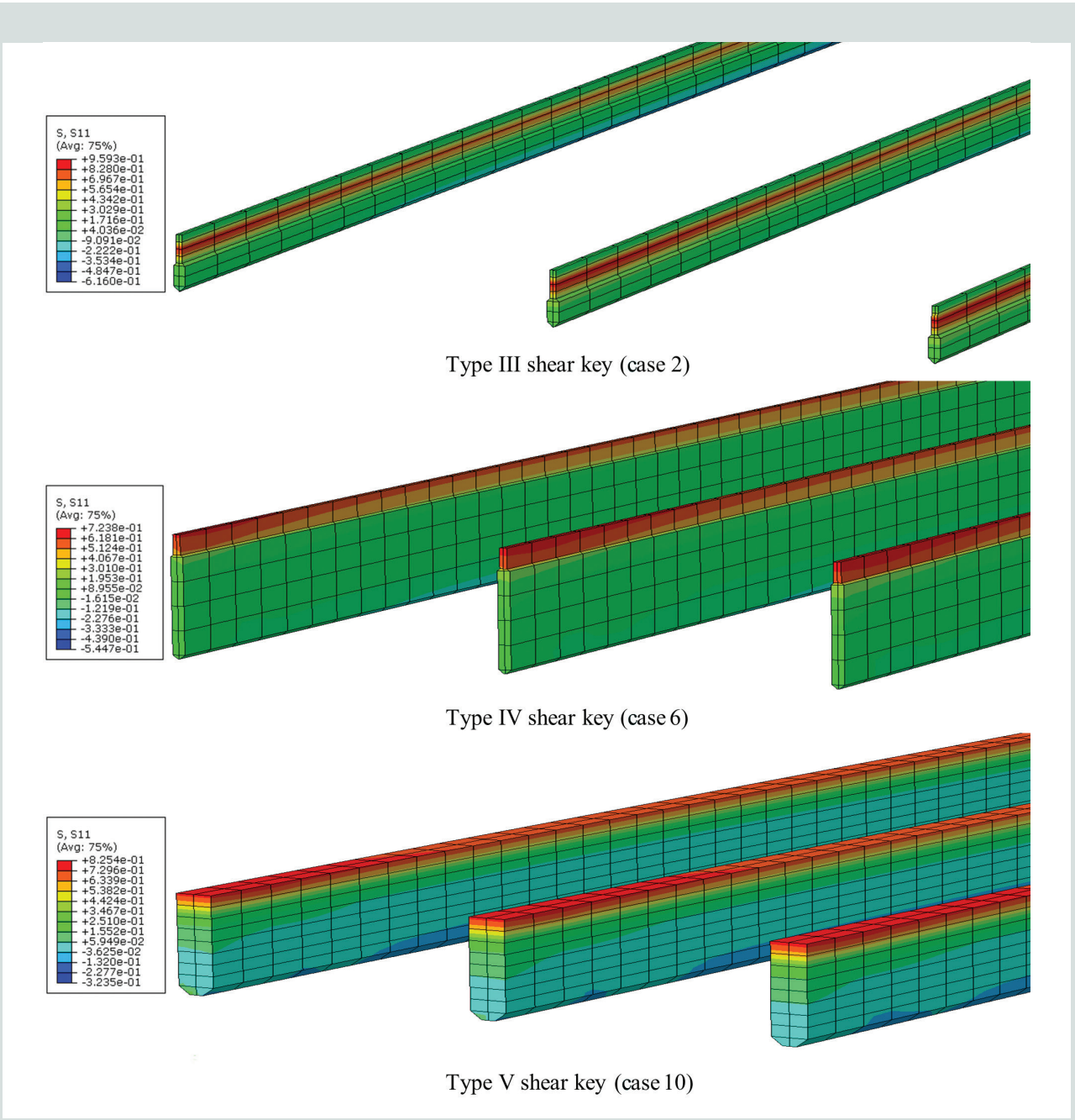

Figure 4. Transverse stress, psi, in shear keys. Note: Color coding reflects the intensity of the stresses with red (+) being tension and blue (-) being compression. S, S11 is notation used by the software to differentiate the stresses in the global axes directions. Avg = average. 1 psi = 6.895 kPa.

Post-tensioning analysis

It has been suggested that lateral post-tensioning can be used to compress the shear keys and mitigate cracking. This was investigated. Note that the investigation was limited to the ability of post-tensioning to mitigate cracking. Other possible benefits of post-tensioning, such as improved load transfer, were not investigated.

Table 1 provides models investigated for post-tensioning analysis. Post-tensioning stresses were applied to provide an average force of 11 to 12 kip (44.5 to 53.4 kN) per linear foot of girder. It was assumed that the post-tensioning is applied as soon as the grout hardens. Thus, the model will be in the condition of having the temperature profile when the post-tensioning is applied. Post-tensioning was simulated by modeling a single 1.5 in. (38 mm) diameter steel bar at the points indicated in Table 1 for post-tensioning models. The bars were post-tensioned by applying an initial strain to the system. Diaphragms, each 18 in. (457 mm) thick, were provided in all the girders at the post-tensioning points to prevent crushing of the webs.

Post-tensioning analysis was run in following steps:

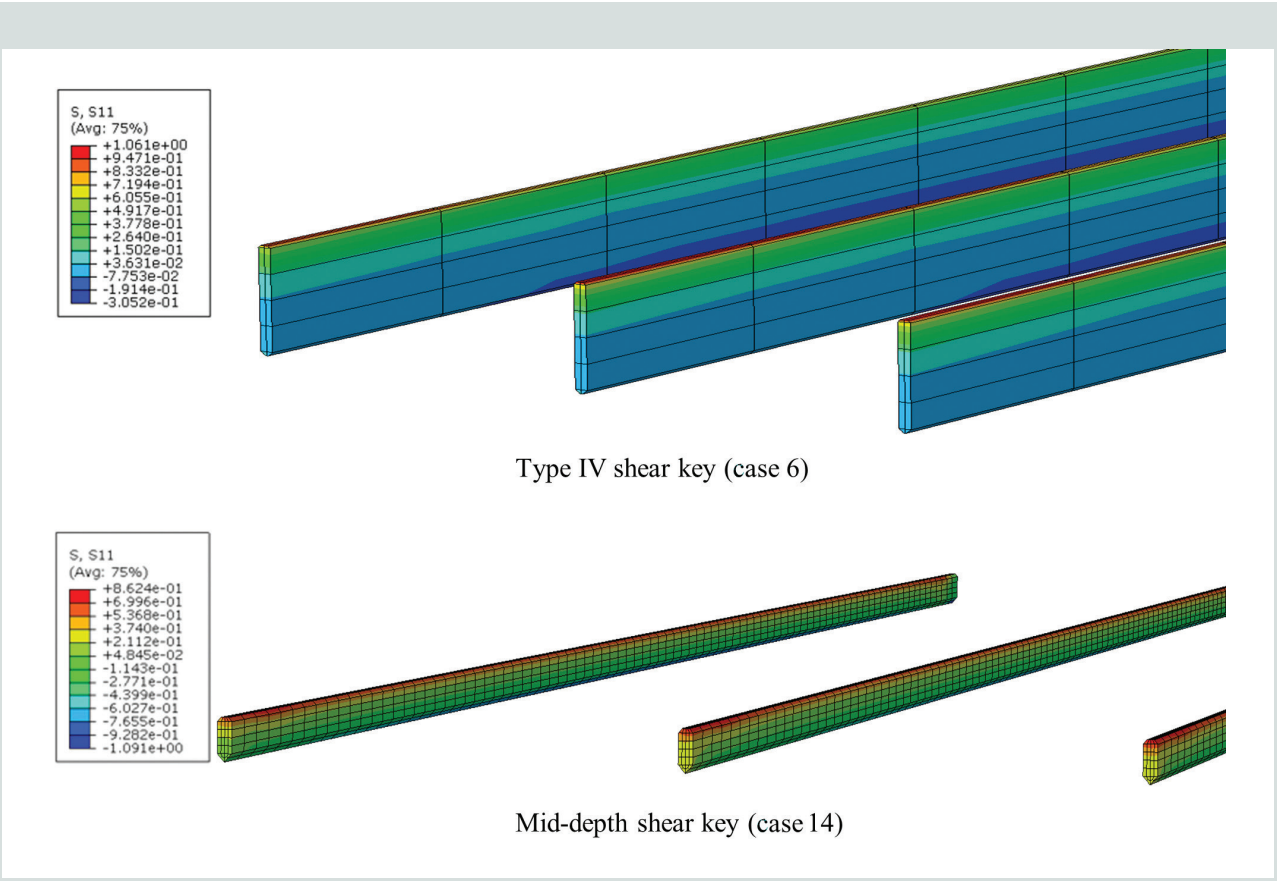

Figure 5. Transverse stress, psi, in shear keys without throat. Note: Color coding reflects the intensity of the stresses with red (+) being tension and blue (-) being compression. S, S11 is notation used by the software to differentiate the stresses in the global axes directions. Avg = average. 1 psi = 6.895 kPa.

1. The bridge was modeled. The shear keys and concrete deck (for models with a concrete deck) were present but were "turned off" to allow the elements to follow the deformations of the girders.

2. The temperature gradient for zone 1 from the AASHTO LRFD bridge design specifications was applied to the box girders. This caused the top of the boxes to expand.

3. The shear key and deck material were then "turned on" to simulate the casting of the shear keys and deck. For asphalt decks, the asphalt was not modeled but the weight was added.

4. Post-tensioning was applied and stresses in shear keys were recorded. This stage helped in determining how the post-tensioning stresses distribute through the bridge, determining the stress profile of shear keys due to post-tensioning alone without any contribution from temperature stresses, and accessing any shear lag through the system.

5. The temperature gradient was then removed from the girder to simulate cooling of the girders.

6. Stresses in shear keys were recorded after cooling. This stage provided the combined effect of post-tensioning and temperature-induced stresses in shear keys.

Post-tensioning stresses only This section presents the result of post-tensioning analysis before the thermal gradient was removed. Because post-tensioning was performed when the thermal gradient was already present, these results show the stress contribution of post-tensioning alone.

As noted in the literature, post-tensioning was most beneficial near the application location and dropped off rapidly away from the post-tensioning locations. This was also observed in the post-tensioning models. The top image in **Fig. 6** shows this effect for post-tensioning application at model ends and midspan. Results for post-tensioning at model ends and third points are shown in the middle image of Fig. 6 and the bottom image of Fig. 6 shows results for post-tensioning application at model ends and quarter points. The figures show the compressive transverse stresses at the point of application of the post-tensioning and before cooling. As can be seen in the figures, the compressive stresses were high at the application of the post-tensioning (ends, midspan, third point, and quarter point), but decreased away from the post-tensioning application. In general, the stress condition shown in the figures was very similar to the condition found in analysis by Lopez de Murphy et al.[16] and is consistent with field measurements[21] and laboratory measurements.[11]

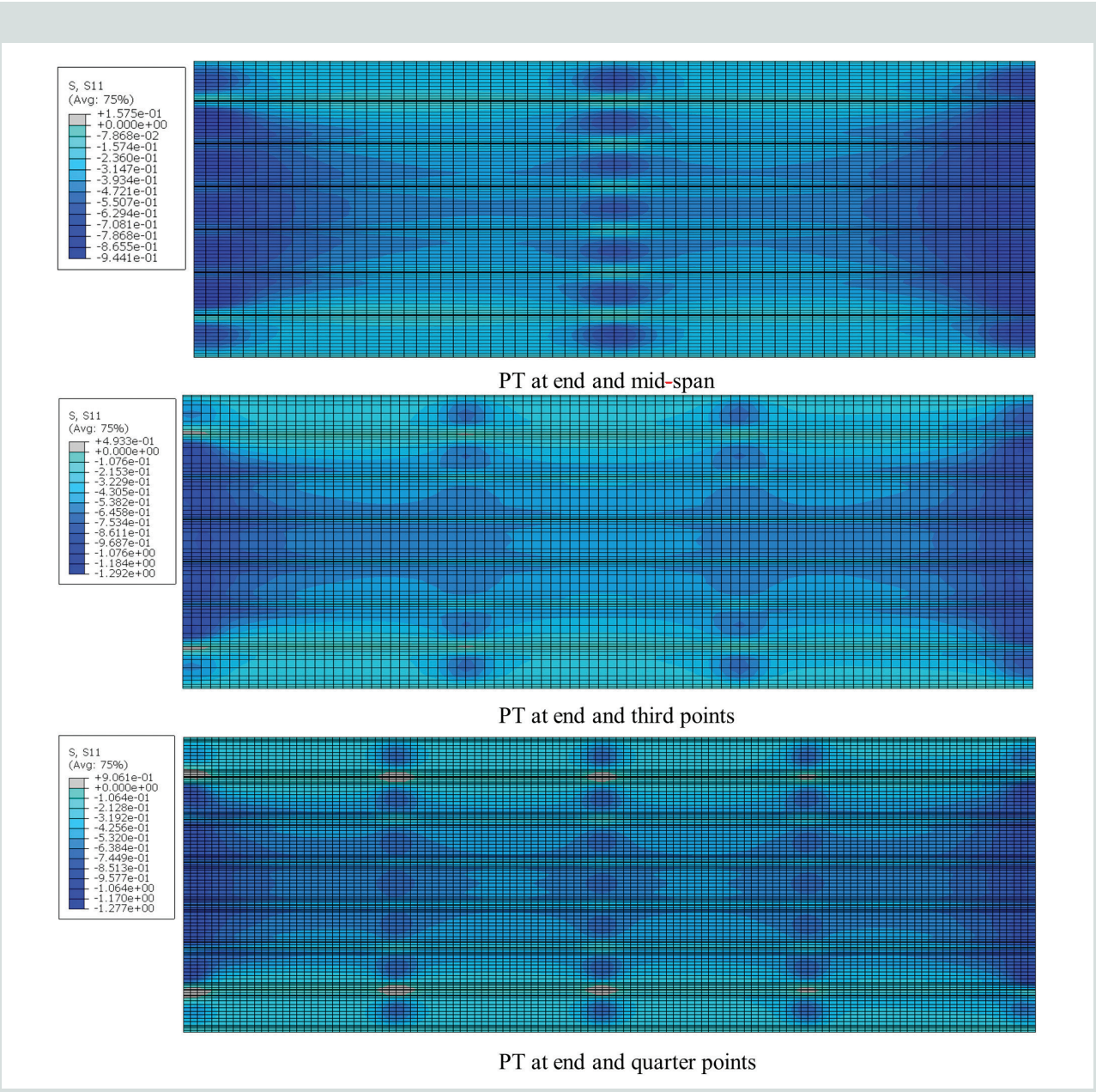

Figure 6. Transverse stress, psi, due to post-tensioning (PT). Note: Color coding reflects the intensity of the stresses with red (+) being tension and blue (-) being compression. S, S11 is notation used by the software to differentiate the stresses in the global axes directions. Avg = average. 1 psi = 6.895 kPa.

Figure 7 shows the left exterior key and two interior keys and how the post-tensioning compresses the shear keys when post-tensioning is applied at the model ends and midspan. For the Type III shear key, the interior keys developed slight compressive stresses throughout the key, while the exterior key developed slight tensile stresses at locations between post-tensioning application points. The highest magnitude of compressive stress developed at the bottom of the key and at points of post-tensioning application. For the Type IV shear key, compressive stresses developed in most key locations, except at the middepth edges of the key, where slight tensile stresses developed. The compressive stresses were greatest at post-tensioning application points and rapidly decreased between post-tensioning points. For the Type V shear key, the distribution of compressive stresses was like the compressive stress distribution of the Type IV key. However, the stresses were lesser in magnitude and tensile stresses were not developed in the key. For the middepth shear key, the compressive stresses were developed at most locations along the key, except at locations between post-tensioning application points where slight tensile stresses developed at the top of the key. The highest compressive stresses developed at points of post-tensioning application.

Combining temperature and post-tensioning stresses

The results of post-tensioning analysis after the thermal gradient was removed are presented here. These results reflect the combined effects of post-tensioning and thermal stresses.

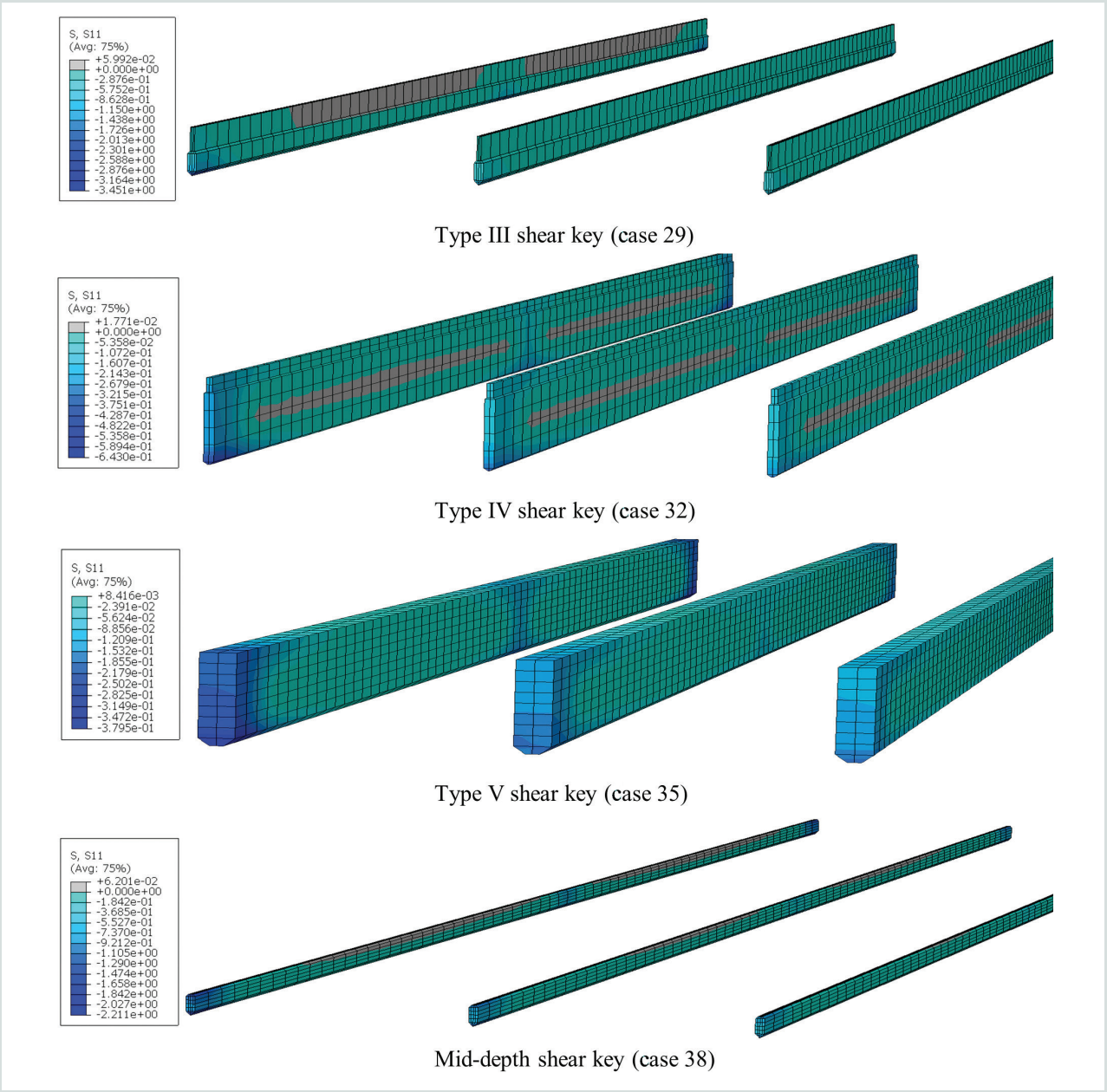

Figure 7. Transverse compressive stress, psi, in shear keys after post-tensioning application. Note: Color coding reflects the intensity of the stresses with red (+) being tension and blue (-) being compression. S, S11 is notation used by the software to differentiate the stresses in the global axes directions. Avg = average. 1 psi = 6.895 kPa.

The maximum stresses in post-tensioned shear keys due to temperature for cases 29 to 44 are presented in Table 3. The maximum transverse stresses occurred at the end of the girders, except for the middepth shear key, in which maximum stresses occurred at midspan. In all cases, the stresses in the transverse direction of the shear keys were higher than those of the longitudinal direction. This agrees with what has often been observed in the field with cracking occurring longitudinally due to transverse stress.

It was observed that the maximum transverse stress in the shear keys increased with the span length and girder depth for the Type III shear keys. However, the maximum transverse shear key stresses decreased with the span and beam depth for the Type IV and Type V shear keys. There was little change for the middepth shear key. When the concrete deck was replaced with an asphalt wearing surface, the maximum transverse stress in the shear keys decreased for all types of shear keys except for the Type III key.

The post-tensioning Type III (standard) key developed lower final maximum transverse tensile stresses compared with the non-post-tensioned Type III key for the shorter span lengths and girder depths. The non-post-tensioned Type III key developed lower final maximum transverse tensile stresses compared with the post-tensioned Type III key at the longer span

length and girder depth. Thus, post-tensioning was less effective for the traditional Type III keys as the girders got longer and deeper. The post-tensioned Type IV, Type V, and middepth keys developed lower final maximum transverse tensile stresses compared with the non-post-tensioned Type IV key for all combinations of span length and girder depth.

While the comparison of maximum transverse tensile stress values between the non-post-tensioned and post-tensioned models may indicate that post-tensioned models generally perform better, this may be misleading as the maximum tensile stress for non-post-tensioned models occurred at the ends, whereas for post-tensioned models, the post-tensioning created compressive stresses and therefore reduced the effective stresses at these locations. Therefore, a more complete assessment was to compare stresses at a fixed location along the shear key for both non-post-tensioned and post-tensioned models. For selected models, transverse tensile stresses were compared at the quarter point of non-post-tensioned and post-tensioned models (**Table 4**). Post-tensioned models with post-tensioning applied at midspan and third points were considered. The results indicated that the post-tensioning did not substantially decrease stresses and in some models increased stresses, as shown in Table 4. Therefore, while post-tensioning may be effective in decreasing the maximum transverse stress experienced by the shear key at post-tension application locations, it was not as effective at decreasing high transverse stresses at locations between the post-tension application points and may even be detrimental.

Reinforced joint analysis

Limited information exists regarding reinforcement in the joint. Most of these designs have used ultra-high-performance concrete as the joint material to allow for shorter embedment lengths of the bars in the joints. Designs have used boxed-out sections for the reinforcement to be installed rather than a continuous reinforcement system. **Figure 8** shows the reinforcement layout for Type III and Type V shear keys. A 12 in. (305 mm) wide by 3 in. (76 mm) deep section of the top flange was removed (boxed out), exposing the no. 4 (13M) reinforcing bars embedded in the flange spaced at 18 in. (457 mm). These reinforcing bars were lap spliced by placing another no. 4 reinforcing bar across the shear key. A lap splice prevents construction conflicts that may arise if flange reinforcement is extended beyond the side of the box to constitute shear key reinforcement.

Table 1 provides the reinforced joint models that were investigated (cases 45 to 48). The reinforced joint models were subjected to the same temperature cycle as the other models and detailed in the previous sections. The models also used the same end diaphragm and bearing pad layouts.

Table 4. Maximum transverse stress in key at locations away from post-tensioning application points

Case	Shear key type	Analysis type	Transverse stress at quarter point from end with one bearing pad, ksi	Change in transverse stress due to post-tensioning, ksi
1	Type III	temp.	0.550	+0.046
29		PT-mid.	0.596	
2	Type III	temp.	0.734	+0.098
30		PT-⅓ pt.	0.832	
5	Type IV	temp.	0.831	-0.019
32		PT-mid.	0.812	
6	Type IV	temp.	0.569	-0.029
33		PT-⅓ pt.	0.540	
9	Type V	temp.	0.712	-0.006
35		PT-mid.	0.707	
10	Type V	temp.	0.711	-0.019
36		PT-⅓ pt.	0.692	
13	middepth	temp.	0.607	+0.041
38		PT-mid.	0.648	
14	middepth	temp.	0.647	+0.016
39		PT-⅓ pt.	0.663	

Note: PT-mid. = models with post-tensioning at ends and midspan; PT-⅓ pt. = models with post-tensioning at ends and third points; temp. = models without post-tensioning. Note: 1 ksi = 6.895 MPa.

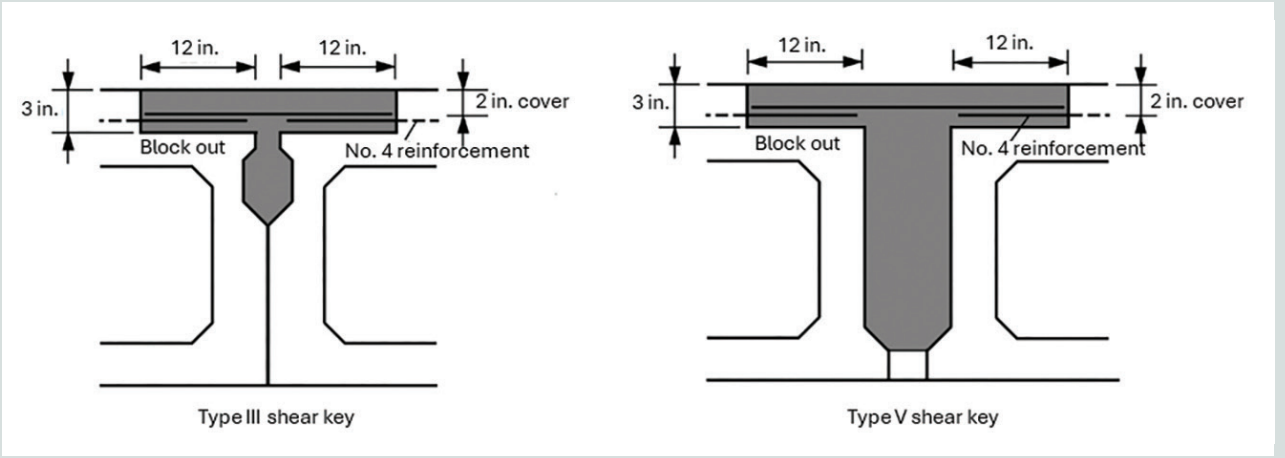

Figure 8. Reinforced shear key layout. Note: See Fig. 1 for shear key dimensions. No. 4 = 13M; 1 in. = 25.4 mm.

The maximum shear key stresses for cases 45 to 48 with reinforcement in the joints are provided in Table 3. The maximum stresses typically occurred at the end of the girders supported by two bearing pads (location II). Stresses in the transverse direction were once again higher than stresses in the longitudinal direction.

Reinforcing the Type III shear key models (cases 45 and 46) resulted in a maximum transverse stress decrease of less than 100 psi (690 kPa) while also resulting in an increase of maximum longitudinal stress. Reinforcing the Type V shear key models (cases 47 and 48) resulted in an increase of both maximum transverse and longitudinal stresses compared with the unreinforced models.

The top image in **Fig. 9** shows the transverse shear key stresses for the reinforced Type III shear key. Stresses were high near the top of the blockout, exceeding 800 psi (5516 kPa), and decreased quickly with depth. While the high transverse stresses near the top of the blockout would likely create crack-

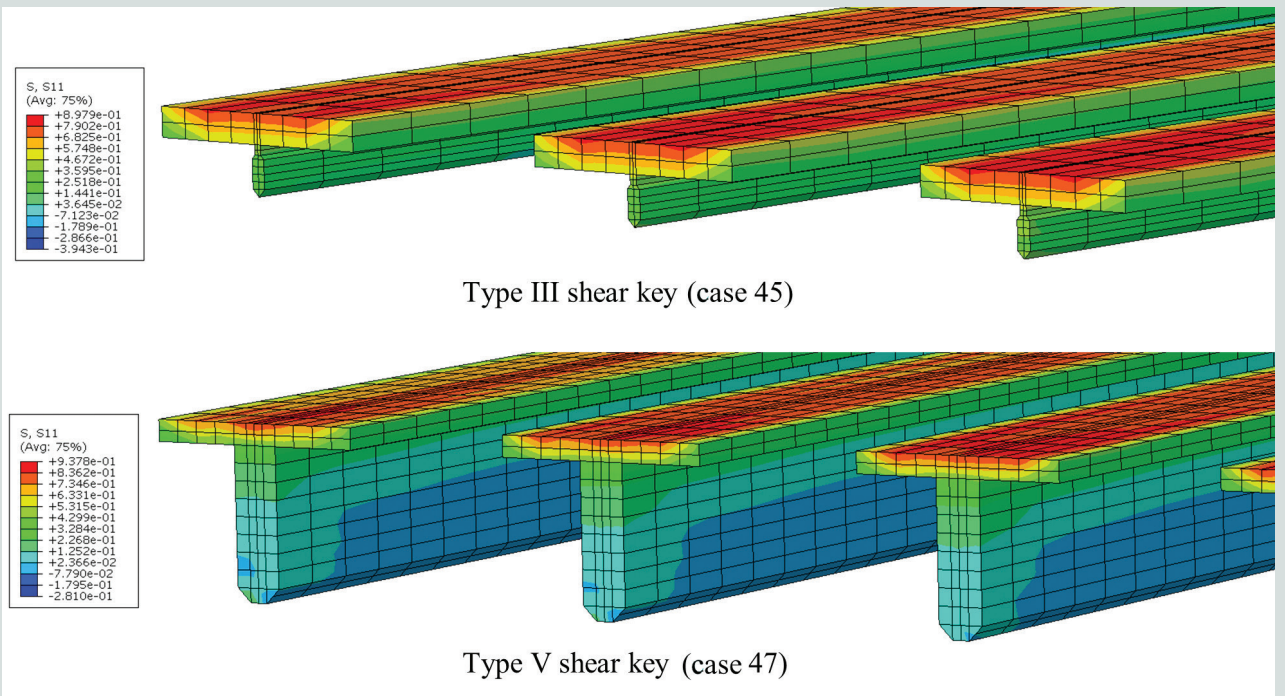

Figure 9. Transverse stress, psi, in reinforced shear keys. Note: Color coding reflects the intensity of the stresses with red (+) being tension and blue (-) being compression. S, S11 is notation used by the software to differentiate the stresses in the global axes directions. Avg = average. 1 psi = 6.895 kPa.

ing near the top, the rapid drop of stresses through the depth of the key may indicate that the cracks would not penetrate any further than the blockout. Compressive transverse stresses were present at the bottom of the key but were of a lesser magnitude than those observed in the unreinforced Type III shear key models. The reinforcing bar developed higher tensile stresses at the ends of the models and at locations embedded in the blockout, with maximum stresses generally not exceeding 9 ksi (62 kPa).

The bottom image of Fig. 9 provides the results for the transverse shear key stresses of the Type V shear key. As observed in the unreinforced Type V key, tensile stresses were high near the top of the blockout and decreased with depth. The high transverse tensile stresses on the top surface of the blockout indicate cracking; however, the rapidly decreasing stresses through the depth of the key may indicate that the cracking did not extend past the blockout. Minor compressive stresses developed near the middepth of the key, but at a lesser magnitude than was observed in the unreinforced Type V key. As observed in the previous models, the embedded reinforcing bar developed higher tensile stresses at the model ends and at locations embedded in the blockout. However, the reinforcing bar stress did not exceed 8 ksi (55 kPa).

Reinforcing the shear key does not seem to help with temperature effects, but it will transfer load if the keys crack. The problem is that reinforcement is placed at the point of maximum temperature movement, so cracking is likely. Bars do not prevent cracking but simply limit the crack width. There is no guarantee that the bars can limit the width enough to prevent leakage.

Live-load analysis

Selected models that were analyzed for temperature stresses were also analyzed separately for vehicular live loads to assess the effect of live load only. An AASHTO HL-93 truck load was placed along the span of the bridge to create the maximum bending moment in the bridge (**Fig. 10**). The maximum tensile stresses in shear keys due to live load only were considerably lower than the tensile stresses due to thermal variations. The maximum transverse stress in shear keys due to live load was less than 11% of the maximum

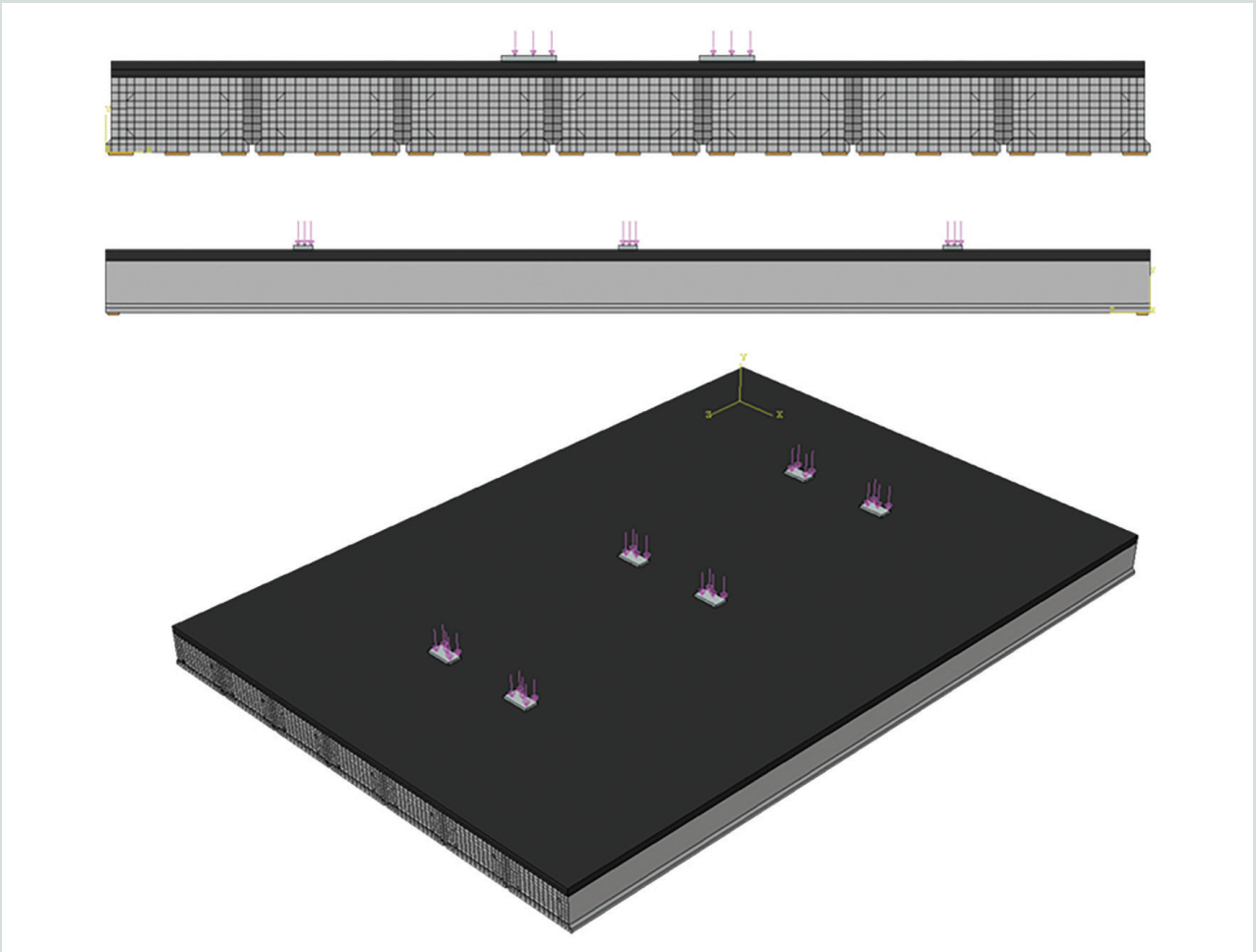

Figure 10. AASHTO HL-93 live load placement on the bridge assembly. Note: AASHTO = American Association of State Highway and Transportation Officials.

transverse stress due to thermal variations for all the cases. The stress in the longitudinal direction was less than 21% of the stress due to thermal loads. In addition, it is interesting to note the stress distribution in shear keys due to live loading. The top image of **Fig. 11** shows the stress distribution in the Type III shear key due to live load only. The stress was mostly compressive, with the tensile stress developing near midspan at the bottom of the shear key. This stress distribution was the opposite of the stress distribution due to temperature. The bottom image of Fig. 11 shows a similar result for the Type IV shear key without the throat grouted. This suggests that the stress distribution due to live load, in addition to being lower, is also opposite of the stress distribution due to thermal variations. Therefore, instead of contributing to the tensile stresses at the top of shear keys, the live-load stresses would alleviate the overall maximum stress in shear keys. However, because the live load is not always present over the bridge, the maximum stresses due to thermal stresses alone would govern the design. Because the live load stresses were low and the stress distribution was opposite to the temperature stress distribution, any further analysis was not seen as being beneficial or yielding useful results.

Conclusion

- The finite element model analysis showed that the temperature stresses were, by far, the largest stresses. Live-load stresses were fairly small in comparison and tended to act in the opposite direction of the temperature stresses. This confirms previous research concluding that temperature cracks the shear keys, that live-load stress alone will not crack the shear keys, and that live load simply drives existing temperature-induced cracks.

- The Type IV (thin full depth), Type V (thick full depth), and middepth shear keys were all superior to the current Type III shear key. Type III developed tensile stresses throughout its depth due to temperature. The middepth shear key developed much lower stress due to being at the point where temperature movements were lowest. The Type IV and Type V shear keys developed high tensile stress at the top, but it quickly diminished with depth. Near the bottom, the stresses were compressive.

- If the throats of Type IV and Type V are not grouted, high tensile stresses develop only at the very top of key. The majority of the key is either in a very low state of tension or in compression. The middepth shear key did not have a grouted throat and exhibited a similar behavior. If the throat of a shear key is not grouted, it could be filled with a material that would provide additional protection against leakage.

- There is no significant effect of girder span, girder depth, or skew angle on the performance of the shear keys.

- Lateral post-tensioning is ineffective at compressing the shear keys to prevent cracking. Confirming field, laboratory, and previous analytical studies, the post-tensioning compressed the shear keys at the point where the

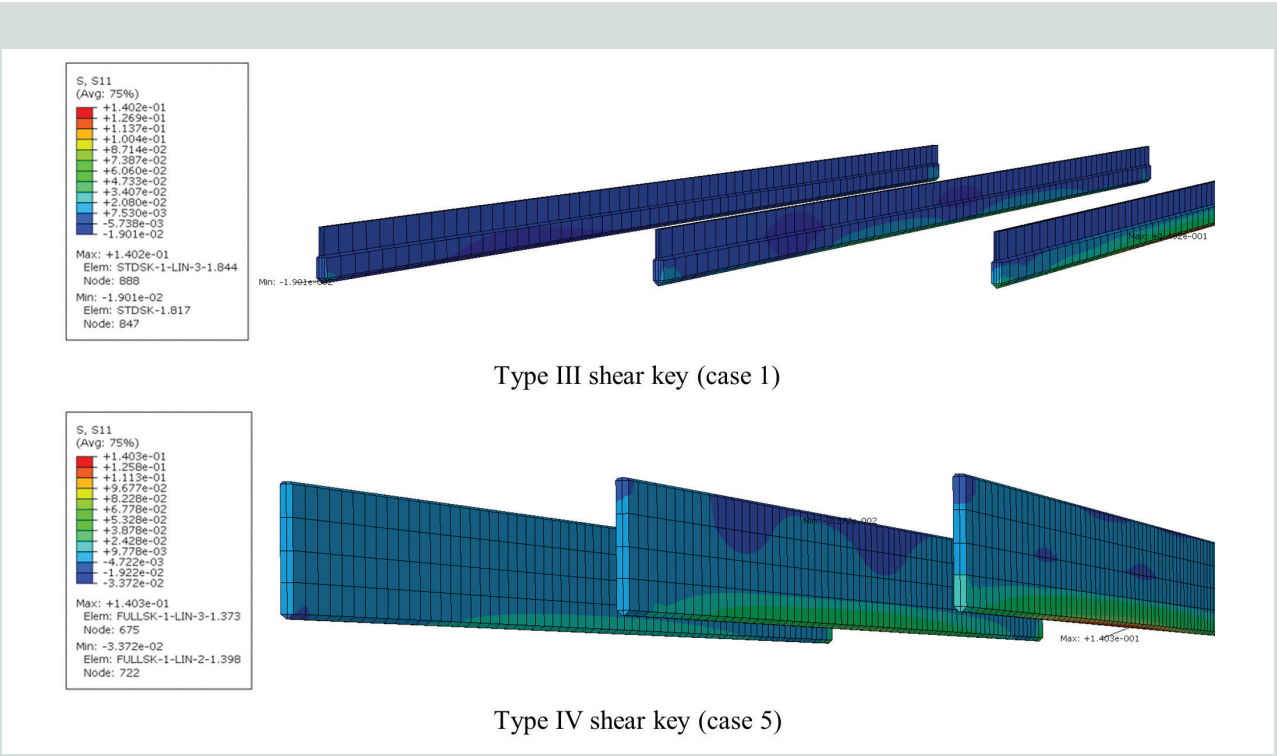

Figure 11. Stress, psi, in shear keys due to live load only. Note: Color coding reflects the intensity of the stresses with red (+) being tension and blue (-) being compression. S, S11 is notation used by the software to differentiate the stresses in the global axes directions. Avg = average; Max = maximum; Min = minimum. 1 psi = 6.895 kPa.

post-tensioning was applied, but the effect diminished quickly away from the point of post-tensioning application. In some cases, additional tensile stresses developed in the shear keys. However, there may be benefits to lateral post-tensioning, such as improving load transfer, that were not investigated here.

- Reinforced joints do not help with temperature stresses but would transfer load. However, these joints are in the region of maximum temperature stress. The joint will likely crack, and the reinforcing bar will not prevent this. The bar may only limit the crack width. This alone cannot guarantee the joint will not leak.

Acknowledgments

The research presented in this paper was a part of the National Cooperative Highway Research Program (NCHRP) project 12-95A, which was documented in Miller et al.[22] The authors wish to thank the NCHRP Project Panel and the senior program officers, Ahmad Abu-Hawash and Waseem Dekelbab, for their project oversight and valuable insight and feedback throughout the project. The material presented in this paper is reproduced with permission from the Transportation Research Board.

References

1. Huckelbridge, Arthur A., Hassan El-Esnawi, and Fred Moses. 1995. "Shear Key Performance in Multibeam Box Girder Bridges." *Journal of Performance of Constructed Facilities* 9 (4): 271–85. https://doi.org/10.1061/(asce)0887-3828(1995)9:4(271).

2. Russell, H. 2009. "NCHRP Synthesis 393, Adjacent Precast Concrete Box Beam Bridges: Connection Details." Washington, DC: National Cooperative Highway Research Program, Transportation Research Board.

3. Fuentes, J. B. 2002. "Structural Condition Assessment and Service Load Performance of Deteriorated Pretensioning Deck Beam Bridges." PhD Dissertation, University of Illinois. Urbana, IL.

4. Steinberg, Eric, Richard Miller, Douglas Nims, and Shad Sargand. 2011. "Structural Evaluation of LIC-310-0396 and FAY-35-17-6.82 Box Beams with Advanced Strand Deterioration." Executive summary report FHWA/OH-2011/16. Columbus, OH. https://rosap.ntl.bts.gov/view/dot/23490/dot_23490_DS1.pdf

5. EI-Remaily, Ahmed, Maher K. Tadros, Takashi Yamane, and Gary Krause. 1996. "Transverse Design of Adjacent Precast Prestressed Concrete Box Girder Bridges." *PCI Journal* 41 (4): 96–113. https://doi.org/ 10.15554/pcij.07011996.96.113

6. Hussein, Husam H., Shad M. Sargand, Anwer K. Al-Jhayyish, and Issam Khoury. 2017. "Contribution of Transverse Tie Bars to Load Transfer in Adjacent Prestressed Box-Girder Bridges with Partial Depth Shear Key." *Journal of Performance of Constructed Facilities* 31 (2): 04016100. https://doi.org/10.1061/(asce)cf.1943-5509.0000973.

7. Miller, Richard A., George M. Hlavacs, Todd Long, and Andreas Greuel. 1999. "Full-Scale Testing of Shear Keys for Adjacent Box Girder Bridges." *PCI Journal* 44 (6): 80–90. https://doi.org/10.15554/pcij.11011999.80.90.

8. Sharpe, Graeme Peter. 2007. "Reflective Cracking of Shear Keys in Multi-Beam Bridges." MS thesis, Texas A&M University.

9. Ulku, Evren, Upul Attanayake, and Haluk M. Aktan. 2010. "Rationally Designed Staged Posttensioning to Abate Reflective Cracking on Side-by-Side Box-Beam Bridge Decks." *Transportation Research Record*, no. 2172 (January): 87–95. https://doi.org/10.3141/2172-10.

10. Hussein, Husam H., Shad M. Sargand, Issam Khoury, and Anwer K. Al-Jhayyish. 2017. "Environment-Induced Behavior of Transverse Tie Bars in Adjacent Prestressed Box-Girder Bridges with Partial Depth Shear Keys." *Journal of Performance of Constructed Facilities* 31 (5): 1–13. https://doi.org/10.1061/(asce)cf.1943-5509.0001068.

11. Graybeal, B. 2017. "Adjacent Box Beam Connections: Performance and Optimization." FHWA-HRT-17-094. McLean, VA: FHWA (Federal Highway Administration).

12. Grace, Nabil F., Elin A. Jensen, and Mena R. Bebawy. 2012. "Transverse Post-Tensioning Arrangement for Side-by-Side Box-Beam Bridges." *PCI Journal* 57 (2): 48–63. https://doi.org/10.15554/PCIJ.03012012.48.63.

13. Lall, Jyotirmay, Sreenivas Alampalli, and Eugene F. DiCocco. 1998. "Performance of Full-Depth Shear Keys in Adjacent Prestressed Box Beam Bridges." *PCI Journal* 43 (2): 72–79. https://doi.org/10.15554/PCIJ.03011998.72.79.

14. Dong, Xuhua. "Traffic Forces and Temperature Effects on Shear Key Connections for Adjacent Box Girder Bridge." PhD diss., University of Cincinnati, 2002.

15. Kim, Jaeheung, Wonseok Chung, and Jang Ho Jay Kim. 2008. "Experimental Investigation on Behavior of a Spliced PSC Girder with Precast Box Segments." *Engineering Structures* 30 (11): 3295–3304. https://doi.org/10.1016/j.engstruct.2008.04.029.

16. Lopez de Murphy, Maria, Jubum Kim, Zi Sang, and Chao Xiao. 2010. Determining More Effective Approaches

for Grouting Shear Keys of Adjacent Box Beams. FHWA-PA-2010-PSU 014. Harrisburg, PA: Pennsylvania Department of Transportation.

17. Hanna, Kromel, George Morcous, and Maher K. Tadros. 2011. "Adjacent Box Girders without Internal Diaphragms or Post-Tensioned Joints." *PCI Journal* 56 (4): 51–64. https://doi.org/10.15554/PCIJ.09012011.51.64.

18. Greuel, Andreas, T. Michael Baseheart, Bradley T. Rogers, Richard A. Miller, and Bahram M. Shahrooz. 2000. "Evaluation of a High Performance Concrete Box Girder Bridge." *PCI Journal* 45 (6): 60–71. https://doi.org/10.15554/PCIJ.11012000.60.71.

19. AASHTO (American Association of State Highway and Transportation Officials). 2020. *AASHTO LRFD Bridge Design Specifications*. 9th ed. Washington, D.C.: AASHTO.

20. Attanayake, Upul, and Haluk Aktan. 2015. "First-Generation ABC System, Evolving Design, and Half a Century of Performance: Michigan Side-by-Side Box-Beam Bridges." *Journal of Performance of Constructed Facilities* 29 (3): 04014090. https://doi.org/10.1061/(asce)cf.1943-5509.0000526.

21. Miller, Richard A, James A Swanson, Richard Engel, Richard Walters, James Barnhart, and Jamal Nusairat. 2009. "Evaluation of the Effectiveness of the Strategic Initiative 9 Pilot Bridge Concepts." Edited by University of Cincinnati, Department of Civil and Environmental Engineering, E. L. Robinson Engineering, and HNTB Corp. Columbus, OH: Ohio Department of Transportation. https://rosap.ntl.bts.gov/view/dot/37775.

22. Miller, R. A., B. Shahrooz, A. Haroon, E. Steinberg, W. Hamid, A. Chlosta, and C. Slyh. 2023. *Guidelines for Adjacent Precast Concrete Box Beam Bridge Systems*. NCHRP 1026. Washington, DC: National Cooperative Highway Research Program, National Academies of Sciences, Engineering, and Medicine.

Notation

A = dimension dependent on depth of girder (12 in. for girder depths ≥ 16 in. and 4 in. for girder depths <16 in.)

T_1 = thermal gradient at girder surface

T_2 = thermal gradient at 4 in. depth

T_3 = thermal gradient at the bottom of the girder

About the authors

Abdullah Haroon, PhD, is an assistant professor in the Department of Civil Engineering at the University of Minnesota-Duluth.

Waleed Hamid is a lecturer in the Civil Engineering Department at the University of Fallujah in Iraq.

Richard Miller, PhD, PE, is a professor emeritus in the Department of Civil and Environmental Engineering at the University of Cincinnati in Cincinnati, Ohio.

Bahram Shahrooz, PhD, PE, is a professor in the Department of Civil and Environmental Engineering at the University of Cincinnati.

Eric Steinberg, PhD, PE, is a professor in the Department of Civil Engineering at Ohio University in Athens, Ohio.

Abstract

Adjacent box-girder bridges are a cost-effective solution for short-span bridges that require a shallow profile. These bridges use precast concrete hollow boxes erected side by side to create a bridge profile with load transfer between the adjacent girders facilitated by shear keys placed near the top of the section. Transverse post-tensioning is also provided along the span to help with load transfer. However, the traditional partial-depth shear keys are susceptible to thermal cracking. Shear-key cracking can cause leakage and loss of load transfer, leading to corrosion and deterioration of the girders. An analytical study with different shear key configurations was performed to investigate joint performance when subjected to thermal and live loads. The effectiveness of post-tensioning and shear key reinforcement in mitigating shear key cracking was assessed. It was concluded that using full-depth or middepth shear keys can potentially improve the performance of adjacent box-girder bridges, whereas post-tensioning or joint reinforcement is ineffective in leakage prevention.

Keywords

AASHTO, box-girder bridge system, bridge girder, lateral post-tensioning, shear key, thermal gradient.

Review policy

This paper was reviewed in accordance with the Precast/Prestressed Concrete Institute's peer-review process. The Precast/Prestressed Concrete Institute is not responsible for statements made by authors of papers in *PCI Journal*. No payment is offered.

Publishing details

This paper appears in *PCI Journal* (ISSN 0887-9672) V. 70, No. 2, March–April 2025, and can be found at https://doi.org/10.15554/pcij70.2-01. *PCI Journal* is published bimonthly by the Precast/Prestressed Concrete Institute, 8770 W. Bryn Mawr Ave., Suite 1150, Chicago, IL 60631.

Reader comments

Please address any reader comments to *PCI Journal* editor-in-chief Tom Klemens at tklemens@pci.org or Precast/Prestressed Concrete Institute, c/o *PCI Journal*, 8770 W. Bryn Mawr Ave., Suite 1150, Chicago, IL 60631.